Development of the work-hardening rate equations for exact prediction of the flow curves at elevated temperatures : application of OFHC. Copper

Development of the work-hardening rate equations for exact prediction of the flow curves at elevated temperatures : application of OFHC. Copper

DEVELOPMENT OF THE WORK-HARDENING RATE EQUATIONS FOR EXACT PREDICTION OF THE FLOW CURVES AT ELEVATED TEMPERATURES

—— Application to OFHC. copper ——

Kenji NAKANISHI

(Received May 31, 1988)

ABSTRACT

In almost all metal forming processes, such as rolling, extrusion, swaging, and forging etc., both strain-rate and temperature vary during deformation. Experimental results reveal that many metallic materials show a remarkable strain rate dependence of flow stress at warm and hot deformation temperature. The work-hardening rate equation previously proposed by the present author,et al. is available to predict the flow curves under the conditions of varying strain-rate and varying temperature during deformation. The equation consists of the basic work-hardening rate term and the relative dynamic recovery rate term. Dynamic restoration process in high temperature deformation involves, in some cases, work-softening due to dynamic recrystallization, in addition to dynamic recovery. Then, the work-softening term is newly formulated and added to the previous equation, and some supplemental equations required for constructing the computer program of flow curve prediction are also developed by the numerical analysis regarding the experimental flow curves of annealed OFHC copper. Some flow curves are calculated by using the computer program of flow curve prediction with taking into account the effects of both varying strain-rate and varying temperature in upsetting experiments, under either isothermal or adiabatic conditions. Excellent agreement is found when the calculated flow curves are compared with those obtained experimentally.

key words: deformation property, experimental and numerical analysis, work-hardening rate, dynamic recovery, dynamic recrystallization, flow curve prediction program

1. Introduction

Many research papers dealing the mathematical description of deformation resistance have been presented.[1)-6)] The auther et al. proposed the work-hardening rate equation and numerical calculation method for predicting the flow curves by which the effective stress and strain of a material being deformed can be predicted continuously with considering both varying effective strain-rate and varying temperature in a deformation process.[6)-9)]

The work-hardening rate equation consists of the basic work-hardening rate term and the relative dynamic recovery rate term formulated from the rate theory of recovery process. The equation is applied to deformation at above basic temperature. Basic temperature at which the relative dynamic recovery rate is assumed zero is usually set to room temperature when the method is adopted to warm and hot deformation. Some materials such as Copper, Aluminum alloys, Nickel, Fe-Cr-Ni stainless steel, γ-Ferrite etc. having

low stacking fault energy and high activation energy for self diffusion represent the work-softening phenomenon in flow curves due to dynamic recrystallization[9)-11)]. Then, the work-softening rate term due to dynamic recrystallization should be added to the previous work-hardening rate equation for the case. In the present work, some numerical analyses have been performed with refering the experimental flow curves of Copper, and 1) the basic work-hardening rate equation for evaluating the basic work-hardening rate term is developed, 2) the work-hardening rate equation at elevated temperature involving both the dynamic recovery rate term and the work-softening term due to dynamic recrystallization is developed, and 3) some experimental parameters involved in the above two work-hardening rate equations are determined, and those parameters are expressed by the mathematical equations as functions of both strain-rate and temperature. The computer program for predicting the flow curve is constructed with the above equations. Excellent agreements are confirmed between the flow curves predicted by the computer program and those measured by experiment at the same strain-rate conditions as those used as input data for computation.

2. Work-hardening rate equations and initial conditions of numerical calculation

Equation (1) or (2) represents the work-hardening rate equation.

$$(d\sigma/d\varepsilon)_{\varepsilon,\dot{\varepsilon},T}=(d\sigma_m/d\varepsilon)_{\varepsilon,\dot{\varepsilon},To}-(k/\dot{\varepsilon})(\sigma_m'-\sigma)\exp[-\{Q_0-f_0(\sigma)\}/RT]-|(\partial\sigma/\partial\varepsilon)_D| \quad (1)$$

$$(d\sigma/d\varepsilon)_{\varepsilon,\dot{\varepsilon},T}=(d\sigma_m/d\varepsilon)_{\varepsilon,\dot{\varepsilon},To}-(\gamma_o/\dot{\varepsilon})(\sigma_m'-\sigma)\exp(q\sigma^2)-|(\partial\sigma/\partial\varepsilon)_D| \quad (2)$$

where $(d\sigma/d\varepsilon)_{\varepsilon,\dot{\varepsilon},T}$ is the work-hardening rate observed at strain ε, strain-rate $\dot{\varepsilon}$ and temperature T(K), the first term of right hand side equation is the basic work-hardening rate at ε, $\dot{\varepsilon}$ and the basic temperature To(K) at which the second and third terms in right hand side equation are set to zero, (To is the lower limit temperature in applying the work-hardening rate equation.), k the rate sensitivity, σ_m' the basic stress explained later, Q_0 the activation energy for self-diffusion, $f_0(\sigma)$ the functional expression giving amount of reduction of activation energy for dynamic recovery due to stress, R the constant (R= 8.32 J/mol K), and the third term the work-softening rate due to dynamic recrystallization that is formulated in the present work. Equation (2) is rewritten from equation (1) by substituting equations (3) and (4). Equation (4) is the result of the previous investigation.[6)] Then, equation (2) contains only two experimental parameters, (γ_0 and q), in the dynamic recovery term.

$$\gamma_0=k\exp(-Q_0/RT) \quad (3)$$

$$f_0(\sigma)=RTq\sigma^2 \quad (4)$$

Figure 1 shows the schematic illustration representing the initial conditions of numerical calculation for predicting the $\sigma-\varepsilon$ curve by Runge-Kutta-Gill method in which equation (2) is employed. The lower illustration shows some curves giving the variables concerned in the calculation. $\sigma_{mo}-\varepsilon$ curve is the basic temperature flow curve observed at the varying strain-rate to be considered in the calculation and at basic temperature. When the $\sigma_{mo}-\varepsilon$ curve is known data, the value of $(d\sigma_m/d\varepsilon)$ in equation (2) can be calculated by equation (5).

$$(d\sigma_m/d\varepsilon)_{\varepsilon,\dot{\varepsilon},To}=(d\sigma_{mo}/d\varepsilon)_{\varepsilon,\dot{\varepsilon},To} \quad (5)$$

The upper figure encircled by the solid line illustrates some variables on stress and strain concerned in the numerical calculation in strain increment $\Delta\varepsilon$. (In the present caculation, $\Delta\varepsilon=0.004$.) The strain, ε_x, and stress, $(\sigma)_{\varepsilon x}$ are the initial values, ε_i and $(\sigma)_{\varepsilon i}$, respectively. $\varepsilon_i+\Delta\varepsilon$ and $(\sigma)_{\varepsilon i+\Delta\varepsilon}$ are the calculated results (computer output), $\varepsilon_x+\Delta\varepsilon$ and $(\sigma)_{\varepsilon x+\Delta\varepsilon}$.

Basic stress, σ_m', in the strain increment is the terminal stress attained at $\varepsilon_i+\Delta\varepsilon$ by deformation with basic work-hardening rate. Therefore, σ_m' is the stress of $\sigma_m-\varepsilon$ curve at strain, $\varepsilon_i+\Delta\varepsilon$, and can be calculated by equation (6). Working energy required for deformation and temperature rise due to working

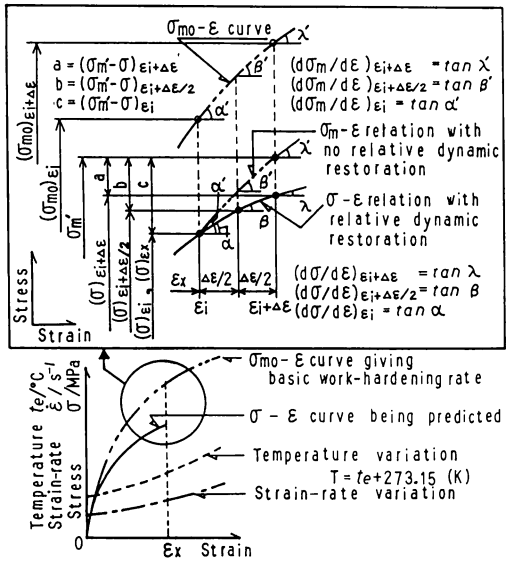

Fig. 1 Graphical expression of some variables concerned in the numerical calculation for predicting the flow curve by using the work-hardening rate equation ($\Delta\varepsilon$: Strain increment in Runge-Kutta-Gill method)

energy in the strain increment, ΔE and Δte, are calculated by equations (7) and (8), respectively.

$$\sigma_m' = (\sigma_{mo})_{\varepsilon i+\Delta\varepsilon} - (\sigma_{mo})_{\varepsilon i} + (\sigma)_{\varepsilon i} \tag{6}$$

$$\Delta E = 0.5(\sigma_{\varepsilon i} + \sigma_{\varepsilon i+\Delta\varepsilon})\Delta\varepsilon \tag{7}$$

$$\Delta te = (\beta\Delta E)/(JC\rho) \tag{8}$$

where β is constant, ($\beta=0$ for isothermal deformation and $\beta=1$ for adiabatic deformation), J the mechanical equivalent of heat ($J=4.2$J/cal), C and ρ specific heat and density of a material, respectively.

In the present work, the basic temperature work-hardening rate equation, equation (9), is introduced so that the basic temperature flow curve at the varying strain-rate being considered can be determined by numerical calculation.

$$(d\sigma_{mo}/d\varepsilon)_{\varepsilon,\dot{\varepsilon},To} = (d\sigma_o/d\varepsilon)_{\varepsilon,\dot{\varepsilon}_b,To} + (\gamma_s/\varepsilon)|(\sigma_o' - \sigma_{mo})|\exp(q_s\sigma_{mo}^2) \tag{9}$$

where the first term in right hand side equation is the work-hardening rate observed at the basic temperature To and at the basic strain-rate $\dot{\varepsilon}_b$, ($\dot{\varepsilon}_b$ should be fixed arbitrarily to some value such as $\dot{\varepsilon}_b=1s^{-1}$.), the second term the relative work-hardening rate (for which, $\gamma_s>0$) or the relative dynamic recovery rate (for which, $\gamma_s<0$), and γ_s and q_s are the experimental parameters. The numerical calculation for predicting the $\sigma_{mo}-\varepsilon$ curve by using equation (9) is performed in the same way as that by using equation (2) and described previously. Values of the first term and σ_o' are calculated by using equations (10) and (11) and the fixed flow curve, $\sigma_b-\varepsilon$ curve. (The flow curve, $\sigma_b-\varepsilon$ curve, should be determined beforehand by experiment at basic strain-rate, $\dot{\varepsilon}_b$, and at basic temperature, To.)

$$(d\sigma_o/d\varepsilon)_{\varepsilon,\dot{\varepsilon}_b,To} = (d\sigma_b/d\varepsilon)_{\varepsilon,\dot{\varepsilon}_b,To} \tag{10}$$

$$\sigma_o' = (\sigma_b)_{\varepsilon i+\Delta\varepsilon} - (\sigma_b)_{\varepsilon i} + (\sigma_{mo})_{\varepsilon i} \tag{11}$$

3. Development of the work-hardening rate equations with refering the experimental flow curves of OFHC copper

3. 1 Experimental data

Some uniaxial compressive tests were performed and the flow curves which are required to determine

the experimental parameters involved in the work-hardening rate equations were prepared. The 7 mm diameter and 10 mm height test pieces are annealed OFHC copper of 99.995 wt% Cu specimens having grain diameter of 0.065mm. Compressive testings were performed by using cam-plastometer. The sub-press containing the testing specimen is heated by the electrical resistance furnace. Specimen's temperature is measured by using the 0.3 mm diameter alumel-chromel thermo-couple and digital pyrometer. The sub-press is taken out from the furnace at slightly higher temperature than the testing temperature and placed on the cam-plasto meter. Then testing is started at the testing temperature. Colloidal graphite (Oil-Dag) is used for lubrication between the tool and specimen interface and for prevention of oxidation of the specimen. Figure 2 shows the flow curves observed by the experiments. Both temperature, te (℃), and strain-rate, $\dot{\varepsilon}$, are constants during deformation. The flow curves are refered in the numerical analysis described below.

3. 2 Procedure and computer program of the numerical analysis

Figure 3 shows some figures illustrating the procedure of the numerical analysis for determining the parameters and terms involved in the work-hardening rate equations. Figure (A) represents the flow curves, $\sigma-\varepsilon$ curve observed at T and $\dot{\varepsilon}$ and $\sigma_{mo}-\varepsilon$ curve at To and $\dot{\varepsilon}$, which are refered from the experimental data shown in figure 2 and used in the analysis.

(1) Determination of the values of γ_0 and q

The values of experimental parameters, γ_0 and q, are determined by the numerical analysis using the equations (12) and (13). Equation (12) is work-hardening rate equation in which both $(\partial\sigma/\partial\varepsilon)_D=0$ and the intermediate experimental parameter, γ, given by equation (13) are substituted into equation (2). Then, equation (12) contains only one experimental parameter.

The m numbers of data pairs, ε_i and σ_i (and $(d\sigma/d\varepsilon)_{\varepsilon i}$ written as Di), are quoted from the experimental data and used in the present analysis. If the flow curve, $\sigma-\varepsilon$ curve, represents work-softening phenomenon due to dynamic recrystallization, the above data pairs are prepared from the flow curve between the strain, $\varepsilon=0$, and the strain at peak stress.

$$(d\sigma/d\varepsilon)_{\varepsilon,\dot{\varepsilon},T}=(d\sigma_m/d\varepsilon)_{\varepsilon,\dot{\varepsilon},To}-(\gamma/\dot{\varepsilon})(\sigma_m'-\sigma) \tag{12}$$

$$\gamma=\gamma_0\exp(q\sigma^2) \tag{13}$$

Figures (B)～(D) show the procedure of the analysis. The solid lines and points plotted with open circles in (B) represent $(d\sigma/d\varepsilon)-\varepsilon$ curves calculated by numerical calculation using the equations (5), (6) and (12) with considering the initial conditions of numerical calculation described in article 2.

The curves are the results obtained by numerical calculation in which some different values of γ, (γ_a, γ_b, ···, γ_g), are substituted into equation (12).

Those γ-values are prepared by equation (14). Equation (14) is introduced so that nearly equi-difference of $(d\sigma/d\varepsilon)$ value between adjacent $(d\sigma/d\varepsilon)-\varepsilon$ curve is achieved at individual strain, ε_i, (plotted by the open circles).

Then, all data is most available to interpolation procedure for determining the value of γ, (γ_i at strain ε_i), by which the same value of $(d\sigma/d\varepsilon)$ as that of experiment can be obtained by the numerical calculation.

$$\gamma=(A\dot{\varepsilon})\log_{10}(M),\ M=1, 2, \cdots\cdots, 7 \tag{14}$$

where A is the constant and can be fixed arbitrarily. ($A=300$ in the present analysis)

Figure (C) shows the procedure for determining the value of γ_i.

The open circles and solid line represents the $(d\sigma/d\varepsilon)-\gamma$ relation prepared from the results shown in figure (B). Refering to the experimental value of work-hardening rate, Di, and $(d\sigma/d\varepsilon)-\gamma$ relation at ε_i, the value of γ_i at ε_i is determined by means of 2nd order polynomial interpolation using the three known

data pairs, $((d\sigma/d\varepsilon), \gamma)$, prepared. In the illustrated case, 2nd order polynomial interpolation is adopted to the data zone II in which the value of Di is contained. Combining σ_i given from the experimental flow curve at ε_i, the data pairs, (γ_i, σ_i), is obtained. The above procedure is performed at all individual strain, ε_i, $i=1$ to m, and m numbers of data pairs are obtained.

If the value of Di is not contained in the $(d\sigma/d\varepsilon)-\gamma$ relation prepared by foregoing numerical calculation, γ_i is determined by extrapolation or larger value of A in equation (14) should be used in the analysis. Figure (D) shows the linear ln γ and σ^2 relation obtained by plotting the data pairs, (γ_i, σ_i^2).

Optimum values of γ_0 and q are determined so that the $\sigma-\varepsilon$ curve calculated by numerical calculation

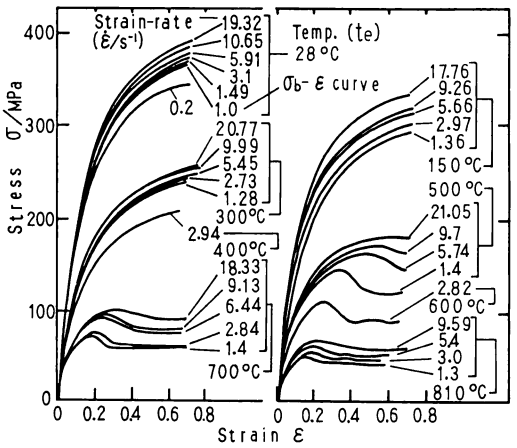

Fig. 2 Experimental flow curves of annealed OFHC copper at some constant strain-rates and at some constant temperatures

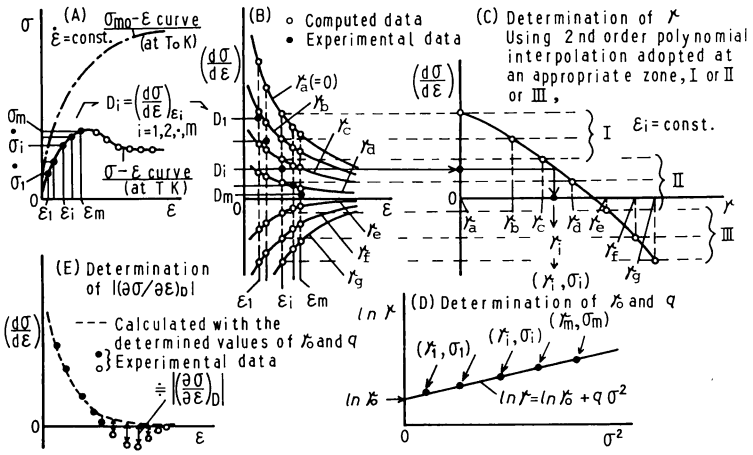

Fig. 3 Figures explaining the sequences of the analytic procedure for determining the parameters, γ_0 and q, and term $|(\partial\sigma/\partial\varepsilon)_b|$ in the work-hardening rate equation

in which the equations representing the $\sigma_{mo}-\varepsilon$ relation, equations (5), (6) and (12) and equation (13) substituted the values of γ_0 and q are employed is best fit to the $\sigma-\varepsilon$ curve observed by experiment.

(2) Determination of $|(\partial\sigma/\partial\varepsilon)_D|$ term

After completion of the determination procedure of the values of γ_0 and q, the values of $|(\partial\sigma/\partial\varepsilon)_D|$ are determined by the numerical analysis.

The experimental values of $(d\sigma/d\varepsilon)$, (expressed with the open circle points in figure (A)), given from the $\sigma-\varepsilon$ curve representing the work-softening phenomenon are refered in the analysis. Difference between the experimental value of $(d\sigma/d\varepsilon)$ and that calculated with considering only dynamic recovery in which both values of γ_0 and q are already determined gives the approximate value of $|(\partial\sigma/\partial\varepsilon)_D|$ at an individual strain as shown in figure (E).

The above differences are used to determine the $|(\partial\sigma/\partial\varepsilon)_D|$ term. The details of the analysis is described in 3・3(3).

(3) Computer program for determining the experimental parameters

Figure 4 shows the interactive computer analysis program which is constructed in accordance with the analysis procedure described in 3.2.(1) and (2). The procedure of correction and optimization of the determined values is also attached to the program. For determination of the experimental parameters, γ_s and q_s, in equation (9), the same computer program, in which the equations (9), (10), (11) are used instead of the equations (2), (5), (6) and the procedure for determining the $|(\partial\sigma/\partial\varepsilon)_D|$ term is omitted, is prepared.

Variable parameter, $\gamma\{\gamma=\gamma_s\exp(q_s\sigma_{mo}^2)\}$, in the program is positive value for $\dot{\varepsilon}>\dot{\varepsilon}_b$, while negative for $\dot{\varepsilon}<\dot{\varepsilon}_b$. ($\gamma=0$ at $\dot{\varepsilon}=\dot{\varepsilon}_b$).

3. 3 Results of analysis

To=301 K(28℃) and $\dot{\varepsilon}_b=1\ s^{-1}$ are set as the basic temperature and basic strain-rate respectively, and the analysis using the computer program shown in figure 4 is performed.

(1) $\sigma_b-\varepsilon$ curve, and computer program for predicting the $\sigma_{mo}-\varepsilon$ curve

The values of γ_s and q_s in equation (9) are determined by refering the $\sigma-\varepsilon$ curves observed at $te=$ 28℃ in figure 2. The results reveals that the value of γ_s is dependent of $\dot{\varepsilon}$ and $q_s=0$. Then, equation (9) is simplified as equation (15). Figure 5 presents the data representing the σ_b and ε relation, ($\sigma-\varepsilon$ curve observed at $te=28$℃ and $\dot{\varepsilon}=1\ s^{-1}$ in figure 2), and the relation between γ_s and $\dot{\varepsilon}$ obtained by the present analysis. (γ_s at $\dot{\varepsilon}<1.49$ are shown by the normal scale.) The $\sigma_b-\varepsilon$ curve is used in the numerical calculation by expressing the segmental 2nd order polynomial equations. The $\sigma_b-\varepsilon$ curve at $\varepsilon>0.7$ is given by $\sigma_b=384.6\varepsilon^{0.165}$. Equations (16) give the mathematical representation of γ_s that are installed in the computer program for predicting the $\sigma_{mo}-\varepsilon$ curve.

$$(d\sigma_{mo}/d\varepsilon)_{\varepsilon,\dot{\varepsilon},To}=(d\sigma_o/d\varepsilon)_{\varepsilon,\dot{\varepsilon}_b,To}+(\gamma_s/\dot{\varepsilon})|(\sigma_o'-\sigma_{mo})| \tag{15}$$

$$\begin{aligned}
\dot{\varepsilon}\geqq 1.49 \quad & \gamma_s=\exp\{-0.0995(\ln\dot{\varepsilon})^2+2.0553(\ln\dot{\varepsilon})+1.4988\}\\
0.7\leqq\dot{\varepsilon}<1.49 \quad & \gamma_s=19.277(\ln\dot{\varepsilon})^2+17.389(\ln\dot{\varepsilon})\\
0.2\leqq\dot{\varepsilon}<0.7 \quad & \gamma_s=-0.278(\ln\dot{\varepsilon})^2+0.452(\ln\dot{\varepsilon})-3.553\\
\dot{\varepsilon}<0.2 \quad & \gamma_s=-5.0
\end{aligned} \tag{16}$$

The computer program for predicting the $\sigma_{mo}-\varepsilon$ curve is constructed with the equation representing the $\sigma_b-\varepsilon$ relation and the equations (10), (11), (15) and (16). Input data of the program is the strain-rate variation in deformation process. The program is installed in the analysis program shown in figure 4 and also the flow curve prediction program described later as the subroutine program. The program can also be used for predicting the $\sigma_{mo}-\varepsilon$ curve of the material having different initial grain diameter when two

procedures described below are added. (i) The procedure for determining the values of σ_b at some strains as shown in figure 5 for the material having specific grain diameter by applying the Hall-Petch relations,[12] and (ii) the procedure to construct the segmental 2nd order polynomial equations for $\varepsilon \leqq 0.7$ and power equations for $\varepsilon > 0.7$ representing σ_b and ε relation.

(2) γ_0 and q

Figure 6 shows the values of γ_0 and q with regard to the values of te (or T) and $\dot{\varepsilon}$. Figure (A) presents the relations between ln γ_0 and ln $\dot{\varepsilon}$.

The relations can be expressed by equation (17).

$$\gamma_0 = \dot{\varepsilon}^{Ca} \exp(Cb) \tag{17}$$

where both Ca and Cb are the temperature dependants.

Figure (B) shows the relation between Ca and te, and the functional expression of the relation for computer program is given by equation (18).

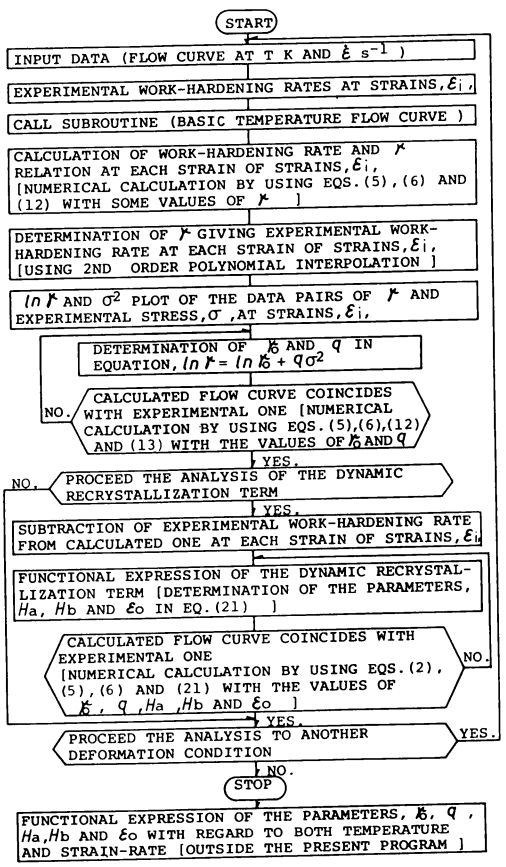

Fig. 4 Flow chart of the interactive computer program used for determining the parameters, γ_0 and q, and term $|(\partial\sigma/\partial\varepsilon)_D|$ in the work-hardening rate equation

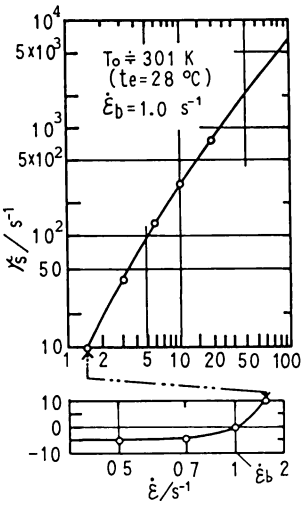

$\sigma_b - \varepsilon$ curve data

Refer to Fig. 2

ε	σ /MPa
0.0	0.0
0.02	39.2
0.04	78.4
0.07	129.4
0.1	161.7
0.13	198.0
0.16	222.5
0.18	236.2
0.20	248.9
0.23	266.6
0.26	282.2
0.3	297.9
0.34	309.7
0.37	319.5
0.4	325.4
0.45	334.2
0.5	343.0
0.55	349.9
0.6	354.8
0.65	359.7
0.7	362.6

Fig. 5 $\sigma_b - \varepsilon$ curve data and $\gamma_s - \dot{\varepsilon}$ relation

Figure (C) gives the relation between Cb and te that can be expressed by equation (19) for computer program.

$te>600$ (℃) $\quad Ca=0.95$

$te\leqq 600$ (℃) $\quad Ca=387.05\times10^{-11}te^3-594.6\times10^{-8}te^2+272.76\times10^{-5}te+0.618$ (18)

$$Cb=2.6436te^{0.1036} \tag{19}$$

The parameter, q, is dependent to T but not to $\dot{\varepsilon}$, and given by equation (20) as shown in figure (D).

$$q=0.0104\exp(-5340.7/\mathrm{T}) \tag{20}$$

(3) $|(\partial\sigma/\partial\varepsilon)_D|$ term

Figure 7 presents the examples explaining the analysis for determining the values of $|(\partial\sigma/\partial\varepsilon)_D|$ term.

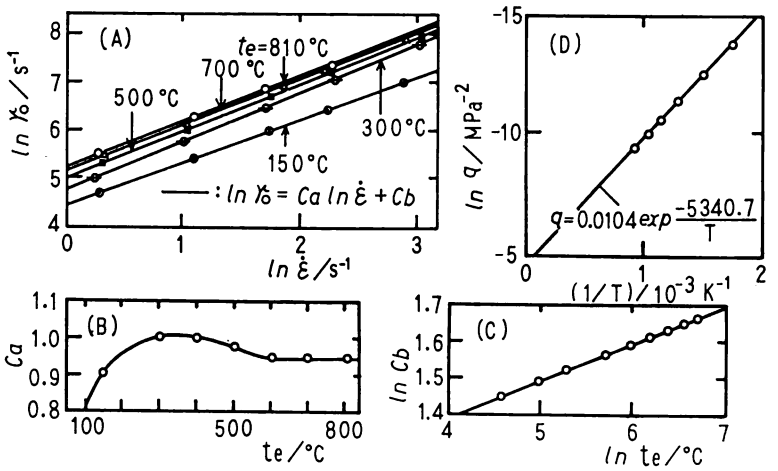

Fig. 6 Both strain-rate, $\dot{\varepsilon}$, and temperature, te, dependence of the parameter, γ_0, and temperature, T, dependence of the parameter, q

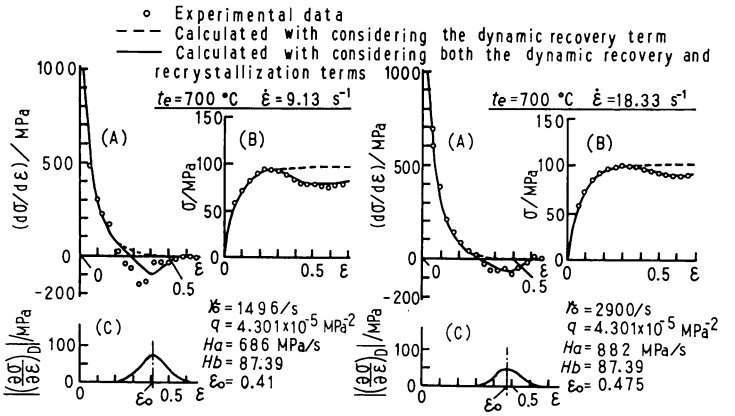

Fig. 7 Examples of the analysis for determining the dynamic recrystallization term, $|(\partial\sigma/\partial\varepsilon)_D|$

The broken lines in figures (A) and (B) are the $(d\sigma/d\varepsilon)-\varepsilon$ curve and $\sigma-\varepsilon$ curve calculated numerically by using equation (2) in which previously determined values of γ_0 and q and $|(\partial\sigma/\partial\varepsilon)_D|=0$ are substituted. While, the open circles plotted in the same figure represent the experimental data.

The differences between the values of $(d\sigma/d\varepsilon)$ observed by experiment and those calculated correspond to the values of $|(\partial\sigma/\partial\varepsilon)_D|$ at individual strains.

Refering to the above differences, the values of $|(\partial\sigma/\partial\varepsilon)_D|$ term at strains of the open circle points are determined and functional expression of the term is investigated. The results of the analysis performed by refering the $\sigma-\varepsilon$ curves at $te\geqq 500$ (℃) in figure 2 reveals that the term $|(\partial\sigma/\partial\varepsilon)_D|$ can be expressed by equation (21). The values of experimental parameters, Ha, Hb and ε_0 involved in equation (21) are also determined in the present analysis.

$$|(\partial\sigma/\partial\varepsilon)_D|=(Ha/\dot{\varepsilon})\exp\{-Hb(\varepsilon-\varepsilon_0)^2\} \tag{21}$$

The values of Ha, Hb and ε_0 could be determined directly by refering the equation to the relations between the above difference of work-hardening rate and strain. It is yet required some correction of the values of the parameters (especially of Ha) determined by the above procedure, because the rate of dynamic recrystallization is affected with the work-softening (stress reduction) due to dynamic recrystallization. The computer program shown in figure 4 involves the confirmation and correction procedure in which the flow curve is calculated by using the equations (2) and (21) and compared with the experimental values. Then, optimum values of the parameters, Ha, Hb, and ε_0 are determined by means of 2 to 3 times trial and error method. The solid lines in figure 7, (A) and (B) represent the results of numerical calculation using the values, Ha, Hb and ε_0, written in the figures. Excellent agreements between the calculated $\sigma-\varepsilon$ curves and those observed by experiment can be confirmed. Figure (C) shows the values of $|(\partial\sigma/\partial\varepsilon)_D|$ in the present calculation.

(4) Critical strain hardening energy, Ec

Figure 8 shows the results of analysis concerning the relation between the strain at which dynamic recrystallization occurs and the strain at peak stress. In the present analysis, the strain at which difference is found between the $(d\sigma/d\varepsilon)-\varepsilon$ curve calculated with considering only dynamic recovery and that with considering both dynamic recovery and dynamic recrystallization is ε_c as illustrated in figure (A), and figure (B) shows the results of the analysis. The results are obtained from the above analysis refering to all flow curves observed at temperatures above 500℃ in figure 2. It could be found that the

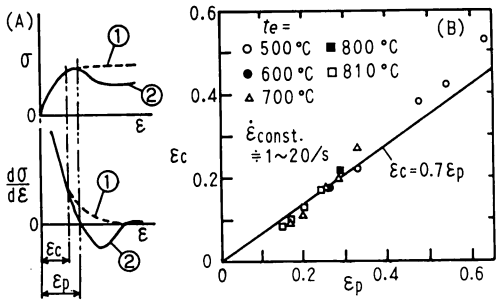

Fig. 8 Strain ε_c, at which restoration due to dynamic recrystallization starts, versus strain ε_p at peak stress
① : Calculated with considering dynamic recovery
② : Calculated with considering both dynamic recovery and dynamic recrystallization

equation, $\varepsilon_c=0.7\varepsilon_p$[9], exists between ε_c and ε_p. Deformation energy required for deformation from $\varepsilon=0$ to ε_c can be considered as the critical value of the energy required for occuring the dynamic recrystallization.[9),10)] Figure 9 shows the relations between Ec and ln $\dot{\varepsilon}$. The relations can be expressed by equation (22).

$$\dot{\varepsilon}<1.0,\ \mathrm{Ec}=e_2\dot{\varepsilon},\quad \dot{\varepsilon}\geqq 1.0,\ \mathrm{Ec}=e_1\ln\dot{\varepsilon}+e_2 \tag{22}$$

where both parameters, e_1 and e_2, are the experimental parameters depending on temperture, te. Relations between the parameters, e_1 and e_2 and temperature, te, are shown in figure (B), and the equations of the relations for computer program are given by equations (23).

$$e_1=\mathrm{Ao}\times10^{-9}te^2+\mathrm{Bo}\times10^{-6}te+\mathrm{Co}\times10^{-4}$$
$$e_2=\mathrm{Do}\times10^{-9}te^2+\mathrm{Eo}\times10^{-6}te+\mathrm{Fo}\times10^{-4} \tag{23}$$

where, $te\geqq750$ (℃) Ao=35.7, Bo=−71.4, Co=366.7,
Do=11.4, Eo=−20.8, Fo=114.4
$650\leqq te<750$ (℃) Ao=−74.8, Bo=83.2, Co=−170.8
Do=121.2, Eo=−184.4, Fo=723.9
$500\leqq te<650$ (℃) Ao=263.0, Bo=−352.3, Co=1232.6
Do=378.0, Eo=−516.9, Fo=1800.2

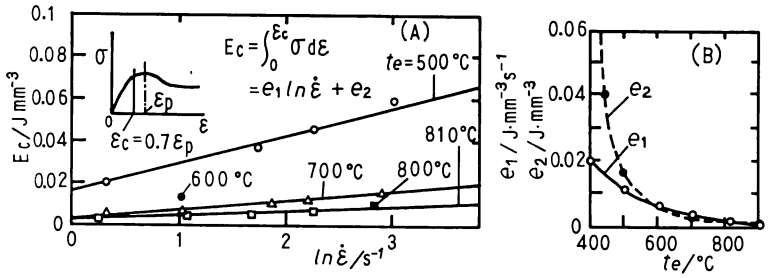

Fig. 9 Both strain-rate, $\dot{\varepsilon}$, and temperature, te, dependence of the critical energy, Ec, required for occuring dynamic recrystallization

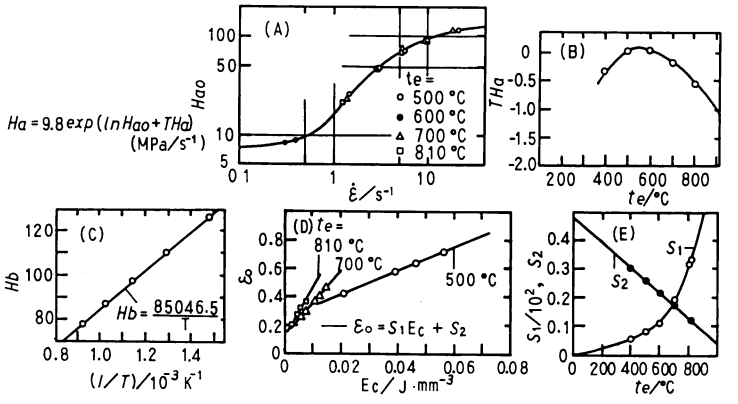

Fig. 10 Both strain-rate, $\dot{\varepsilon}$, and temperature, te, dependences of the parameters, Ha, Hb and ε_0 (Ec: Refer to Fig. 9)

$te<500$ (℃) Ao=300.2, Bo=−342.4, Co=1090.3
Do=7130.5, Eo=−7236.9, Fo=18518.9

(5) The equations giving the values of Ha, Hb and ε_o

Figure 10 shows the results of analysis for constructing the equations expressing the relations between the parameters Ha, Hb and ε_o and the deformation conditions $\dot{\varepsilon}$, te (or T) and Ec. It could be found that ln Ha and $\ln\dot{\varepsilon}$ relations at some constant temperatures represent parallel curves. Then, the relation between Ha and both te and $\dot{\varepsilon}$ can be expressed by equation (24).

$$Ha=9.8\exp(\ln Hao+Tha) \tag{24}$$

where the parameter, Hao, is the dependent to $\dot{\varepsilon}$ and parameter, Tha, to te. Figure (A) represents the relation between Hao and $\dot{\varepsilon}$ and (B) the relation between THa and te. Those relations are expressed by the equations (25) and (26).

$$Hao=\exp\{A_2\times10^{-4}(\ln\dot{\varepsilon})^4+B_2\times10^{-3}(\ln\dot{\varepsilon})^3+C_2\times10^{-3}(\ln\dot{\varepsilon})^2+D_2\times10^{-2}(\ln\dot{\varepsilon})+E_2\} \tag{25}$$

where $\dot{\varepsilon}\geqq1.0$ $A_2=-26.545$, $B_2=31.392$, $C_2=-260.687$,
$D_2=120.442$, $E_2=2.8266$
$\dot{\varepsilon}<1.0$ $A_2=370.936$, $B_2=308.646$, $C_2=936.838$,
$D_2=133.07$, $E_2=2.8235$

$$THa=A_3\times10^{-6}te^2+B_3\times10^{-3}te+C_3 \tag{26}$$

where $te\geqq600$ (℃) $A_3=-6.152$, $B_3=5.707$, $C_3=-1.17$
$400\leqq te<600$ (℃) $A_3=-16.87$, $B_3=18.77$, $C_3=-5.15$
$te<400$ (℃) $A_3=-7.0$, $B_3=11.4$, $C_3=-3.78$

The parameter, Hb, is dependent to T and can be expressed by equation (27) as shown in figure (C).

$$Hb=85046.5/T \tag{27}$$

Figure (D) shows the relations between ε_o and Ec at some temperatures. Those relations can be expressed by equation (28).

$$\varepsilon_o=S_1Ec+S_2 \tag{28}$$

where both S_1 and S_2 are the temperature dependents as shown in figure (E), and can be expressed by equation (29).

$te\geqq500$ (℃) $S_1=251.02\times10^{-6}te^2-246.42\times10^{-3}te+68.8$
$te<500$ (℃) $S_1=15.43\times10^{-6}te^2+8.98\times10^{-3}te$
$S_2=-44.66\times10^{-5}te+0.4831$ (29)

(6) Repetition of dynamic recrystallization process

Figure 11 shows the schematic illustrations explaining repetition of dynamic recrystallization process and an example of the analysis of the phenomenon. Figures (A-1) ~ (A-3) are the illustrations showing the $\sigma-\varepsilon$ curve, variation of strain hardening energy, E, and variation of work-softening, $|(\partial\sigma/\partial\varepsilon)_D|$, in the deformation. Those figures explain that dynamic recrystallization occurs repeatedly whenever work-hardening energy reaches the value of critical energy, Ec. The results of analysis reveals that work-softening rate due to dynamic recrystallization appeared in n'th order can be estimated by equation (30). Equation (30) is given from eq. (21) by multiplying the correction facter $1/4^{n-1}$. Strain ε_o in equation (30) is measured from the strain at which the strain-hardening starts. (Refer to figure 11.)

$$|(\partial\sigma/\partial\varepsilon)_D|=\{(Ha/4^{n-1})/\dot{\varepsilon}\}\exp\{-Hb(\varepsilon-\varepsilon_o)^2\} \tag{30}$$

Figures (B) ~ (D) show the results of analysis with refering to the $\sigma-\varepsilon$ curve observed at $te=700$ ℃ and $\dot{\varepsilon}=1.4s^{-1}$. Figures (B) and (C) show comparisons of the $(d\sigma/d\varepsilon)-\varepsilon$ curve and $\sigma-\varepsilon$ curve obtained by numerical calculation with those observed by experiment respectively. The broken lines are the calculated results in which $|(\partial\sigma/\partial\varepsilon)_D|=0$ is substituted in equation (2), the single dotted lines in which

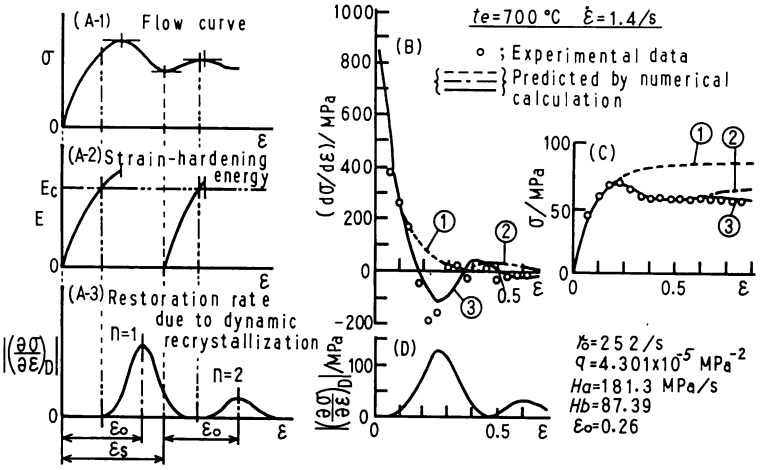

Fig. 11 Interpretation of repetition of dynamic recrystallization
① : Calculated with considering dynamic recovery, ② : Calculated with considering both dynamic recovery and single dynamic recrystallization, ③ : Calculated with considering both dynamic recovery and repeated dynamic recrystallization

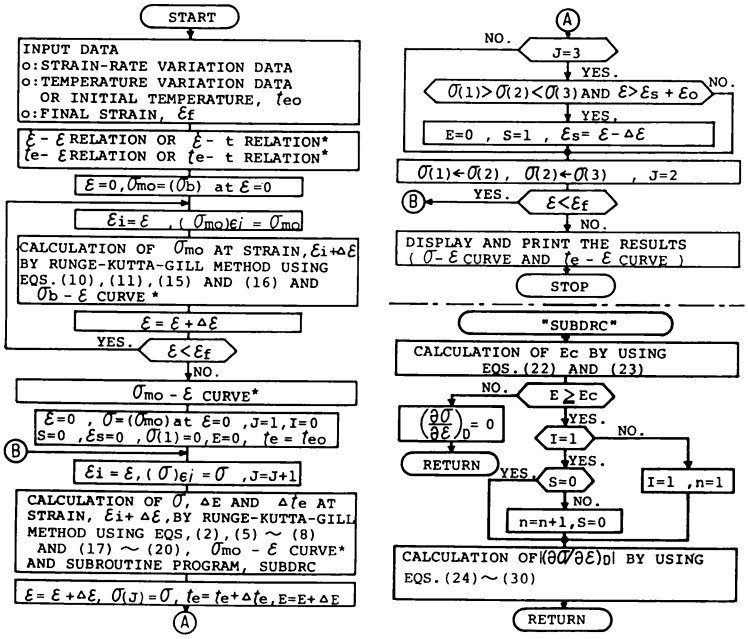

Fig. 12 Flow chart of the computer program for predicting the flow curves
t: Time (s), $\Delta\varepsilon=0.004$, I, J and S: Control parameters of the program
* = Expressed by a series of sectional 2nd order polynomial equations

equation (21) is substituted in equation (2), and the solid lines in which equation (30) is substituted in equation (2). Figure (D) presents the variation of $|(\partial\sigma/\partial\varepsilon)_D|$ calculated by equation (30).

4. Computer program for predicting the $\sigma-\varepsilon$ curves

Figure 12 presents the flow chart of computer program for predicting the $\sigma-\varepsilon$ curves. Input data for computation are strain-rate variation, temperature variation or initial temperature and final strain. Output data are $\sigma-\varepsilon$ curve and temperature variation in the deformation. Figure 13 shows the examples of $\sigma-\varepsilon$ curve predicted by using the computer program, figure 12. Input data are deformation temperature written in the figures and strain rate variation, $\dot{\varepsilon}_v$, shown in the upper figures and observed by upsetting by oil-hydraulic press, {figures (A)-(C)}, and by constant compressive ram speed by cam-plastometer, {figures (D) and (E)}. The solid lines in the lower figures show the $\sigma-\varepsilon$ curves predicted and the open circle points plotted in the same figures represent the stresses at some strains observed by experiments performed under the same deformation conditions used for the computations. Excellent agreements are confirmed between the $\sigma-\varepsilon$ curves predicted and those observed by experiments. Furthermore, some calculation to estimate quantitative effect of the varying strain-rate on $\sigma-\varepsilon$ curve are performed. The single dotted lines and broken lines are the $\sigma-\varepsilon$ curves predicted with considering the constant high strain-rates, $\dot{\varepsilon}_1$, or constant low strain-rates, $\dot{\varepsilon}_2$, which are involved in the individual varying strain-rates, $\dot{\varepsilon}_v$.

The $\sigma-\varepsilon$ curves under the adiabatic deformation conditions are also predicted with considering both varying strain rates and varying temperatures. {$C=0.093$ (cal/g ℃) and $\rho=8.96$ (g/cm³) are substituted in equation (8)}

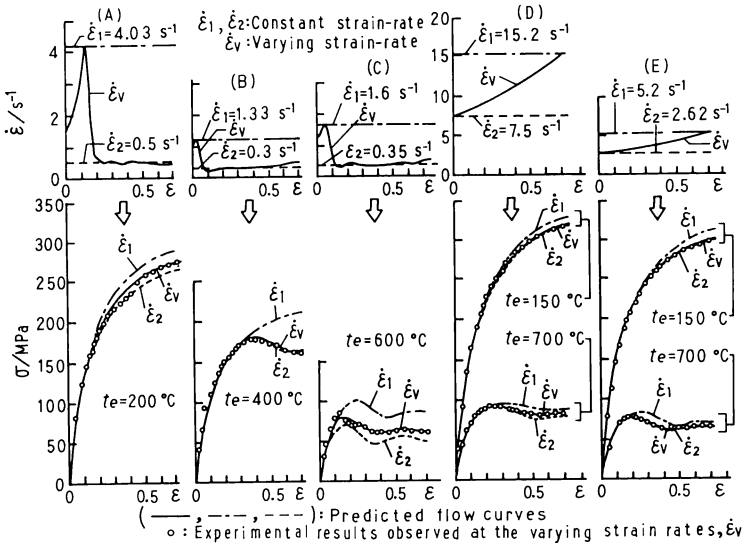

Fig. 13 Examples of the flow curves predicted at three strain-rate conditions, i. e., at two constant strain-rates, $\dot{\varepsilon}_1$ and $\dot{\varepsilon}_2$, and at one varying strain-rate, $\dot{\varepsilon}_v$, in the individual case, (A) – (E), by using the computer program shown in Fig. 12 The points plotted by open circles are the experimental data obtained at the varying strain-rate, $\dot{\varepsilon}_v$, in the individual case, (A) – (E).

Table 1 shows the mutual comparisons of the stresses predicted under the isothermal deformation condition or the adiabatic deformation condition or measured by experiment at three strain values. The strain rate conditions are the same varying strain-rates, $\dot{\varepsilon}_v$, as shown in figure 13.

The $\sigma-\varepsilon$ curves under the adiabatic condition show slightly low stress level compared to those under the isothermal condition. Much remarkable difference between the flow curves under the isothermal condition and those under the adiabatic condition could be predicted in large deformation. (Refer to appendix 2)

Table 1 Comparison of the flow curves measured or predicted by showing the flow stresses at three strains

σ_i :FLOW STRESS PREDICTED IN ISOTHERMAL DEFORMATION
σ_a :FLOW STRESS PREDICTED IN ADIABATIC DEFORMATION
σ_e :FLOW STRESS OBSERVED BY EXPERIMENT
$(te)_a$:DEFORMATION TEMPERATURE IN ADIABATIC DEFORMATION

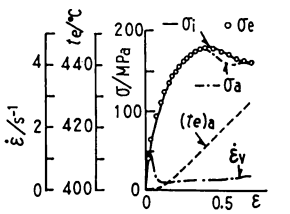

Example of the results
Input data
(Strain rate: $\dot{\varepsilon}_v$,(B) in Fig.13
Temperature: te=400°C)

Input data $\dot{\varepsilon}_v$ and te	Strain ε	Flow stress σ/MPa σ_i	σ_a	σ_e	Temp/°C $(te)_a$
(A) in Fig. 13	0.3	226.8	226.8	218.0	212.6
	0.5	260.0	258.8	258.2	226.5
te=200°C	0.68	273.5	271.8	274.4	240.1
(B) in Fig. 13	0.3	169.9	168.7	168.9	409.5
	0.5	175.2	160.4	171.7	419.2
te=400°C	0.68	157.4	159.3	160.5	427.3
(C) in Fig. 13	0.3	63.0	62.4	69.4	605.4
	0.5	65.8	65.3	62.8	609.0
te=600°C	0.68	64.8	59.8	62.7	612.2
(D) in Fig. 13	0.3	260.6	259.4	264.6	164.3
	0.5	300.4	283.0	297.9	180.3
te=150°C	0.68	317.2	314.0	314.4	196.0
(E) in Fig. 13	0.3	247.2	246.3	245.0	163.6
	0.5	285.0	283.1	280.3	178.8
te=150°C	0.68	300.9	298.2	297.9	193.7
(D) in Fig. 13	0.3	92.9	91.8	92.1	706.1
	0.5	82.2	80.6	83.3	711.0
te=700°C	0.68	83.2	81.4	83.9	715.1
(E) in Fig. 13	0.3	74.7	73.9	71.5	705.4
	0.5	63.4	63.0	66.6	709.0
te=700°C	0.68	68.6	67.6	67.8	712.4

5. Conclusions

Some experimental analyses are performed with refering to the experimental flow curves of annealed OFHC copper. In the present analyses, the work-hardening rate equation that consists of the basic work-hardening rate term, the dynamic recovery rate term and the work softening term due to dynamic recrystallization and the basic work-hardening rate equation that gives the value of basic work-hardening rate term are constructed. It has been reported that the dynamic recrystallization process is strongly affected with the material's structure such as initial grain diameter. The above conditions can be involved in the experimental parameters in the present equations. Application of the method to the other materials requires determination of the experimental parameters involved in the two work-hardening rate equations. This can be achieved easily by using the interactive computer program for determining the values of the experimental parameters in the work-hardening rate equations.

References

1) Kato,K.: J.Materials (材料), 30-330(1981),95.
2) Hartley,C.S.& Srinivasan,R.: Trans.ASME, J.Engng.Mater. & Technol., 105-7(1983),162.
3) Dadras,P.: ibid., 107-4(1985), 97.
4) Hojyo,A., Chyatani,A, Yonetani,S.: J.Materials Sci. (材料科学), 22-2(1985),90.
5) Yada,H. & Senuma,T.: J.Japan Society for Technology of Plasticity (塑性と加工), 27-300(1986),34

6) Okamura,S., Nakamura,T. & Nakanishi,K.: ibid., 16-175(1975),636.
7) Nakanishi,K., Okamura,S. & Nakamura,T.: ibid., 18-203(1977),990.
8) Nakanishi,K., Okamura,S., Fukui,Y. & Nakamura,T.: ibid., 22-246(1981),669.
9) Maki,M. & Tamura,I.: J.Materials, 30-329(1981),107.
10) Sakai,T.: 101th JSTP.Simposium text,(1985),11
11) Nakamura,T. & Ueki,M.: 学振第123委研究報告 18-3(1977),243.
12) Armstrong,R.W.: Advances in Materials Research,4,(1970),101-119, John Willey & Sons, Inc. New York

Appendix 1-Computer analysis

Some CRT. hard copys are presented here according to the order of analysis, so that the intermediate results as well as the whole procedure of the computer analysis for determining the experimental parameters involved in the work-hardening rate equations could be understood. In the construction procedure of the work-hardening rate equations for a metal or an alloy, the basic temperature and basic strain rate should be fixed at first. It should be noted that the basic temperature is the lowest limit temperature at which the work-hardening rate equations are adopted.

While, there is no special restriction in setting the value of the basic strain-rate. In the present case, room temperature is set as the basic temperature by expecting that the work-hardening rate equations are applied in warm and hot deformation and unit strain-rate, 1 s^{-1}, is set as the basic strain-rate. The experimental parameters, γ_s, in the basic work-hardening rate equation should be determined with refering the experimental flow curves which are observed at some constant strain-rates under the basic temperature. Present analysis reveals that the value of q_s in the basic temperature work-hardening rate equation is always 0. Then, determination of the value of γ_s can be performed simply by comparing the experimental flow curve with the flow curves calculated by using equations (9), (10), (11) and the values of γ_s given as input data. Figure 14 is the CRT. hard copy showing an example of the above procedure. Some points representing the experimental flow stresses at some strains are plotted at first on the stress and strain coordinate system in CRT. display. Refering to those experimental data, some flow curves which are available to determine the proper value of γ_s are calculated and displayed on the CRT.

In the present case, four different flow curves shown by the solid lines are calculated by using four different values of γ_s; *i.e.*, γ_s=10, 100, 200 and 300. Then, proper value of γ_s, by which the best fit flow curve to experimental one can be calculated, is determined from the above data.

In the present strain-rate, $\dot{\varepsilon}=5.91/s$, $\gamma_s=139/s$ is determined as the optimum value of γ_s by interpolation procedure applied to the calculated relations between flow stress and γ_s and the experimental flow stresses at some strains. The above interactive computer analysis are performed with refering some experimental flow curves that are measured at some strain-rates, and the equations representing the relation between the value of γ_s and strain-rate, $\dot{\varepsilon}$, is obtained. Then the computer program for predicting the basic flow curve can be constructed with equations (9), (10), (11) and equation giving the value of γ_s. (such as equation (16))

Followed analysis is to determine the experimental parameters of γ_0 and q in the dynamic recovery term and Ha, Hb and ε_o in the dynamic softening term in the work-hardening rate equation at elevated temperature by using the semi-automated interactive computer program presented in figure 4.

The procedure for determining the parameters Ha, Hb and ε_o is omitted for the materials representing only dynamic recovery. The following figures show a series of intermediate and final results obtained in

the analysis for determining the experimental parameters with refering the experimental flow curve at $\dot{\varepsilon}=18.33s^{-1}$ and at 700 ℃. Table 2 presents the computer out put showing the basic temperature flow curve at $\dot{\varepsilon}=18.33s^{-1}$ calculated by the subroutine program that is installed in the present analysis program.

Figure 15 shows the CRT. hard copy representing the $(d\sigma/d\varepsilon)-\varepsilon$ curves, (A), and the $\sigma-\varepsilon$ curves, (B), obtained by the numerical calculations using the equations (5), (6) and (12) with some different values of γ given by equation (14). The plotted points by open circles represent the experimental data. The values of γ at some stresses are determined automatically by the numerical analysis, descrived in 3.2.(1), using the computer.

Figure 16 shows the values of γ at some stresses and CRT. hard copy showing ln γ and σ^2 plots. Then the values of γ_0 and q are determined from the linear relation between ln γ and σ^2, ln $\gamma=\ln\gamma_0+q\sigma^2$.

The optimum values of γ_0 and q are determined by trial and error method so that the best fit flow curve which is obtained by numerical calculation using the equations (5), (6), (12) and (13) to the experimental one is achieved. Figure 17 presents the CRT. hard copy showing confirmation that the values of γ_0 and q

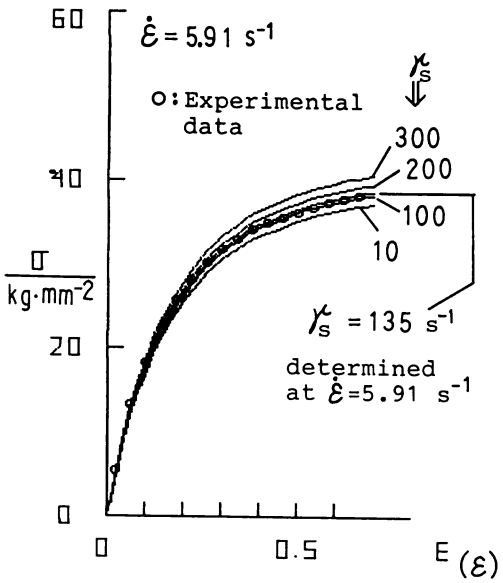

Fig. 14 Example of analysis for determining the values of γ_s at some strain-rates

Table 2 Basic temperature flow curve, σ_{mo}-ε curve, calculated by using the computer program

TIME t (s)	STRAIN ε (-)	STRAIN -RATE ε̇ (1/s)	STRESS σmo (kg/mm²)	STRESS σb (kg/mm²)
T	E	V	Y1	Y1B
0.000	0.000	18.330	0.000	0.000
0.001	0.020	18.330	4.315	4.000
0.002	0.040	18.330	8.633	8.000
0.003	0.060	18.330	12.598	11.678
0.004	0.080	18.330	15.652	14.511
0.005	0.100	18.330	17.839	16.500
0.007	0.120	18.330	20.642	19.100
0.008	0.140	18.330	22.870	21.167
0.009	0.160	18.330	24.522	22.700
0.010	0.180	18.330	26.027	24.100
0.011	0.200	18.330	27.429	25.400
0.012	0.220	18.330	28.747	26.622
0.013	0.240	18.330	29.969	27.756
0.014	0.260	18.330	31.096	28.800
0.015	0.280	18.330	32.015	29.650
0.016	0.300	18.330	32.824	30.400
0.017	0.320	18.330	33.525	31.050
0.019	0.340	18.330	34.118	31.600
0.020	0.360	18.330	34.876	32.311
0.021	0.380	18.330	35.451	32.844
0.022	0.400	18.330	35.837	33.200
0.023	0.420	18.330	36.225	33.560
0.024	0.440	18.330	36.614	33.920
0.025	0.460	18.330	37.002	34.280
0.026	0.480	18.330	37.390	34.640
0.027	0.500	18.330	37.777	35.000
0.028	0.520	18.330	38.105	35.304
0.029	0.540	18.330	38.398	35.576
0.031	0.560	18.330	38.657	35.815
0.032	0.580	18.330	38.881	36.023
0.033	0.600	18.330	39.074	36.200
0.034	0.620	18.330	39.315	36.424
0.035	0.640	18.330	39.522	36.616
0.036	0.660	18.330	39.695	36.776
0.037	0.680	18.330	39.833	36.904
0.038	0.700	18.330	39.936	37.000

are proper ones by comparing the calculated $(d\sigma/d\varepsilon)-\varepsilon$ curve and $\sigma-\varepsilon$ curve with experimental ones, respectively.

(The comparison is valied only in the strain range between 0 to 0.3 in which the restoration process is only dynamic recovery.) Figure 18 shows the CRT. hard copy that represents the further analysis for

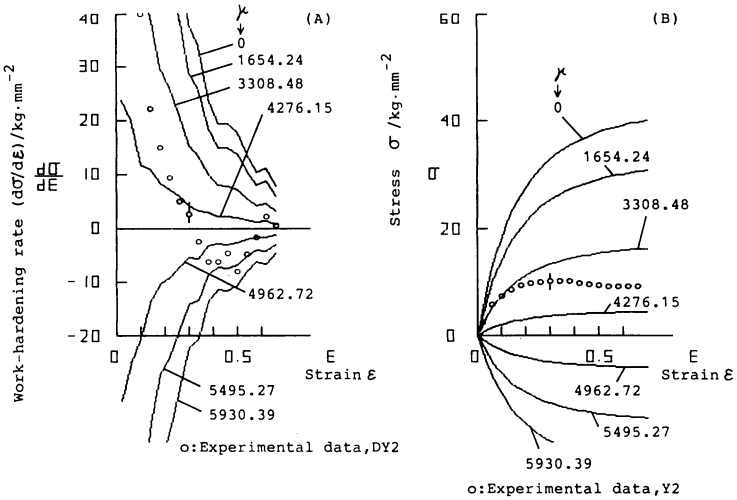

Fig. 15 Computed intermediate data and experimental data for determining the values of γ_0 and q in the work-hardening rate equation Deformation temperature, $te=700℃$, Strain-rate, $\dot{\varepsilon}=18.33\ s^{-1}$

ε	σmo	(dσmo/dε)	σ	(dσ/dε)	σ²	γ
(-)	(kg/mm²)		(kg/mm²)		(kg/mm²)²	(s⁻¹)
E	Y1	DY1	Y2	DY2	Y2*Y2	G
0.060	12.598	175.480	5.845	61.111	34.160	3518.780
0.100	17.839	124.747	7.400	40.000	54.763	3560.470
0.140	22.870	97.015	8.645	22.222	74.729	3918.480
0.180	26.028	72.668	9.400	15.000	88.361	3996.170
0.220	28.746	63.499	9.811	9.445	96.250	4167.230
0.260	31.096	51.149	10.100	5.000	102.002	4330.610
0.300	32.825	37.744	10.300	2.500	106.090	4407.890

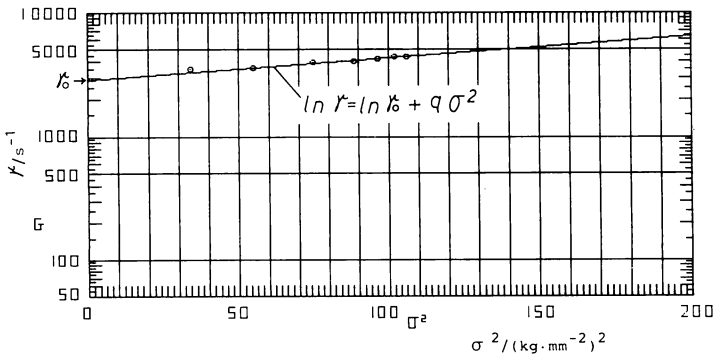

Fig. 16 $\ln\gamma$ and σ^2 plots and determination of γ_0 and q in the work-hardening rate equation Deformation temperature, $te=700℃$, Strain-rate, $\dot{\varepsilon}=18.33\ s^{-1}$

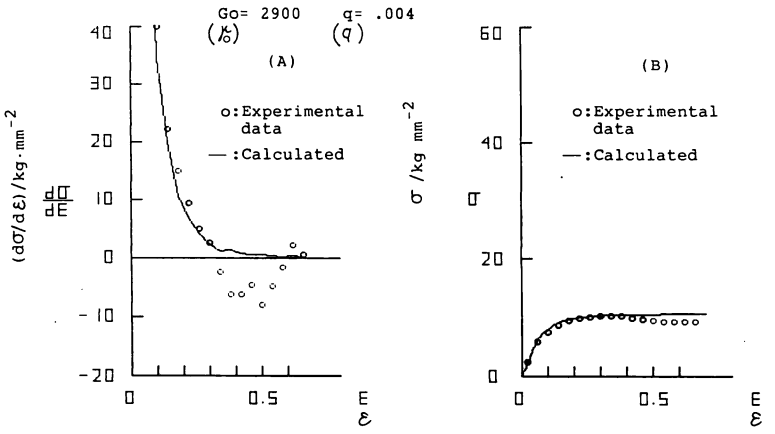

Fig. 17 Confirmation of the values of γ_0 and q determined by the numerical analysis
Deformation temperature, te=700℃, Strain-rate, $\dot{\varepsilon}$=18.33 s^{-1}

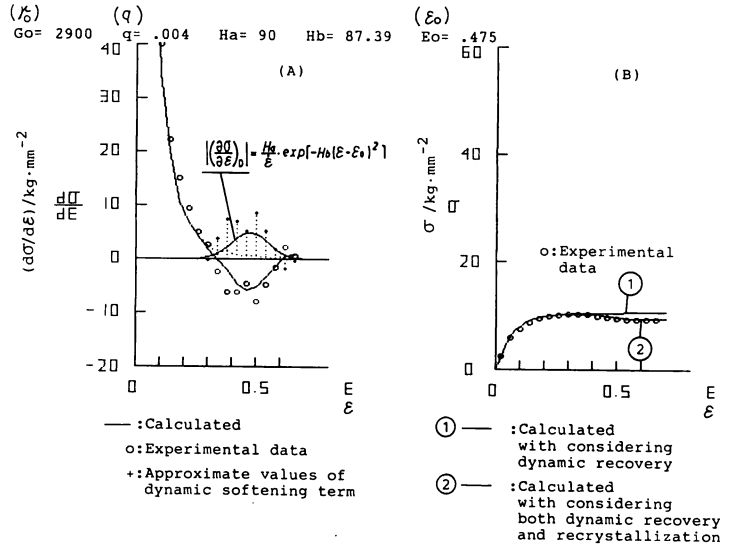

Fig. 18 Analysis for determining the dynamic softening term due to dynamic recrystallization
Deformation temperature, te=700℃, Strain-rate, $\dot{\varepsilon}$=18.33 s^{-1}

determining the values of experimental parameters, Ha, Hb and ε_o in equation (21).

The optimum values of Ha, Hb and ε_o are determined by trial and error method so that the best fit flow curve to the experimental one is calculated by using the equations (2), (5), (6) and (21). Figure (A) shows the approximate values of dynamic softening term at some strains which are used as reference data for the present analysis and $(d\sigma/d\varepsilon)-\varepsilon$ curve for confirmation of the values of experimental parameters. Figure (B) shows mutual comparison between the experimental flow curve and the $\sigma-\varepsilon$ curves calculated with considering only dynamic recovery and with considering both dynamic recovery and dynamic recrystallization. (The optimum values of parameters, γ_o, q, Ha, Hb and ε_o are used in the calculation.)

Figure 19 is the CRT. hard copy representing final confirmation that the values of experimental parameters determined by the present analysis are correct values by comparing the $(d\sigma/d\varepsilon)-\varepsilon$ curve and $\sigma-\varepsilon$ curve calculated with the experimental ones, respectively. (The comparison is valied in whole strain range, because both restoration processes; i.e., dynamic recovery and dynamic recrystallization are taken into account in the calculation.)

Appendix 2-Examples of flow curve prediction in large deformation

Figures 20 and 21 present the CRT. hard copys showing the flow curves predicted up to large strain, $\varepsilon=2.5$, by using the computer program, (figure 12). Figure 20 is the results calculated at constant strain-rates and at constant temperatures. While, figure 21 is the results calculated at two types of varying strain-rates during deformation under the isothermal or adiabatic condition. The strain-rate variation in figure (A) is assumed with expecting a forging and (B) is assumed with expecting a extrusion.

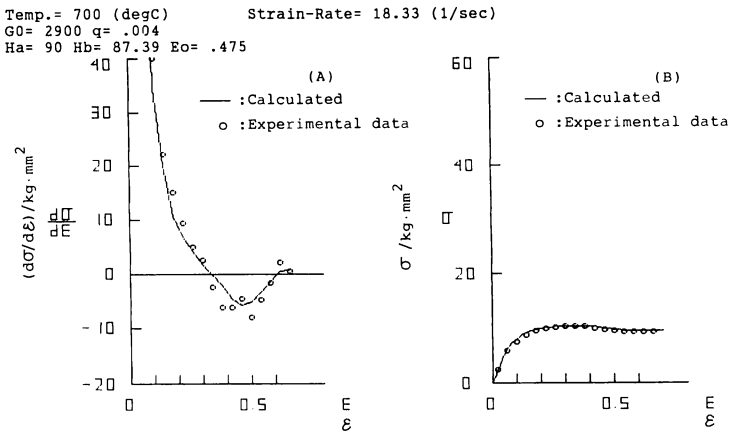

Fig. 19 Final confirmation as well as confirmation of the values of H_a, H_b and ε_0 determined by the numerical analysis

Deformation temperature, $te=700℃$, Strain-rate, $\dot{\varepsilon}=18.33\ s^{-1}$

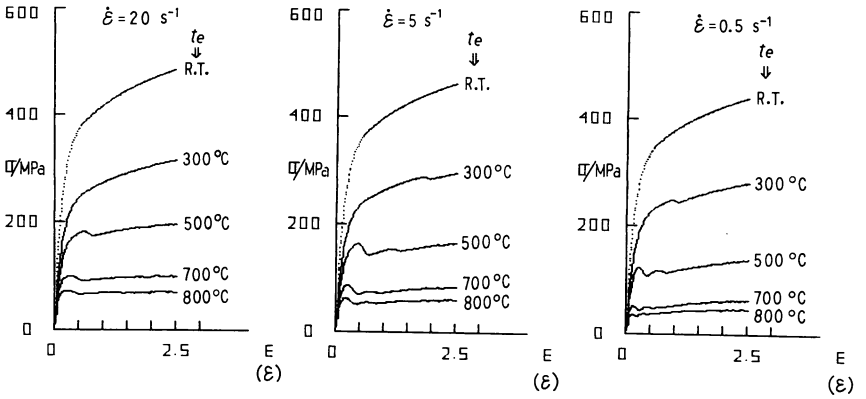

Fig. 20 Some flow curves predicted by the computer program, (Refer to Fig. 12) Both deformation temperature, te, and strain-rate, $\dot{\varepsilon}$, are constants in the deformation. (R. T.: Room temperature assumed as basic temperature)

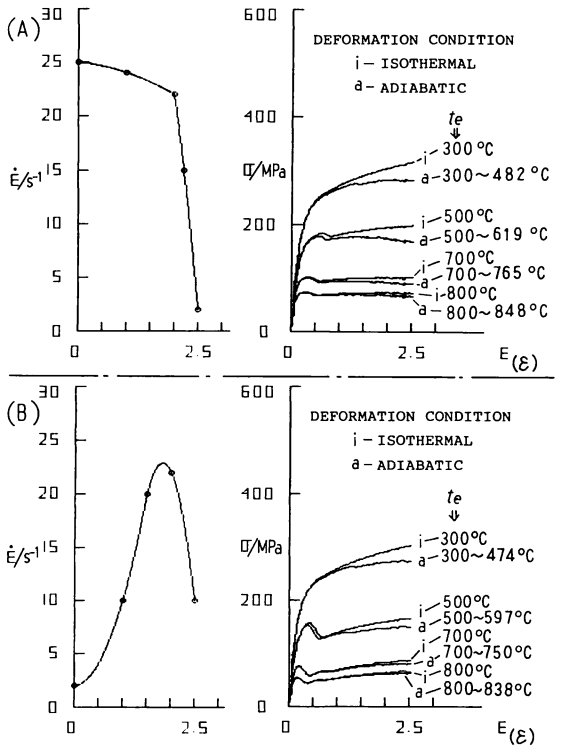

Fig. 21 Some flow curves predicted by the computer program, (Refer to Fig. 12),
Two types of varying strain-rates and isothermal or adiabatic deformation are assumed in the flow curve prediction.